Journal of Polymer Science

WILEY

JOURNAL OF POLYMER SCIENCE

RESEARCH ARTICLE OPEN ACCESS

Fluorene-Arylamine Copolymers: Separable Control of Hole Transport and Light Emission Through Composition and Conformation

Nikol T. Lambeva[1,2] | Saurav Limbu[3] | Ji-Seon Kim[3] | Donal D. C. Bradley[1,4]

[1]Department of Physics, University of Oxford, Oxford, UK | [2]Institute of Ion Beam Physics and Materials Research, Helmholtz-Zentrum Dresden-Rossendorf, Dresden, Germany | [3]Department of Physics and Centre for Processable Electronics, Imperial College London, London, UK | [4]NEOM Education, Research, and Innovation Foundation, Al Khuraybah, Tabuk Province, Saudi Arabia

Correspondence: Nikol T. Lambeva (nikol.lambeva@physics.ox.ac.uk) | Donal D. C. Bradley (donal.bradley@neom.com)

Received: 15 January 2025 | **Revised:** 4 March 2025 | **Accepted:** 6 March 2025

Funding: This work was supported by Engineering and Physical Sciences Research Council (1734270).

Keywords: charge trapping | copolymers | hole transport | mobility | polyfluorenes

ABSTRACT

Suitable model polymer systems enable systematic studies that can progress understanding of structure–property relationships in these chemically diverse materials. To this end, the hole mobility of four fluorene-arylamine copolymers containing varying ratios of 9,9-dioctylfluorene and butyl-substituted phenylenediamine has been studied. The copolymers with longer sequences of fluorene units can adopt the chain-extended β-phase conformation, and its effect on transport is also investigated. The room temperature hole mobility of the fluorene homopolymer, poly(9,9-dioctylfluorene), is drastically reduced by copolymerization of 5% arylamine units due to trapping at the arylamine sites. With increasing arylamine percentage, the mobility rises due to the commencement of direct arylamine-to-arylamine transport. Air photoemission spectroscopy measurements reveal two separate contributions to the photoemission signal whose intensities vary with composition, rather than a single energy level that shifts continuously from fluorene to arylamine, as has sometimes been assumed in transport models. This work demonstrates both that mobility can be controlled over a large range in these copolymers and that the role of fluorene β-phase formation is secondary here to chemical composition. Conversely, the light emission properties are strongly affected by conformation. The transport and emission characteristics are thereby separable, consistent with the observed multifunctional nature of state-of-the-art complex copolymers.

1 | Introduction

Conjugated polymers have been the focus of extensive research, especially since their early demonstration as effective materials for electroluminescence, and subsequently photovoltaic solar energy conversion, with more recent interest also addressing biosensing and photonics functions [1–4]. To facilitate their development for commercial applications, a thorough understanding of the electronic processes in these materials has been required. A large variety of chemical structures has been synthesized, incorporating different building blocks, such as arylene, arylene vinylene, fluorene, thiophene, benzothiadiazole, and arylamine [5, 6]. Copolymerization, where two or more monomers are combined through covalent links [7] offers the advantage of enriching and adjusting material properties without the unwanted phase separation typical of polymer blends [8].

However, to achieve competitive device efficiencies, significant further optimization has been required of both polymer chain composition and architecture, including substituent groups that

provide solubility and simultaneously modulate conformation and solid-state packing [9]. Charge carrier transport determines performance for a number of device types [10], aiding more efficient solar cells, faster switching in field effect transistors, and higher space charge limited (SCL) currents in organic light-emitting diodes. Great efforts have, accordingly, been made to achieve higher mobilities through insight into molecular structure–property relationships and charge transport physics [9, 11, 12].

In relation to the present study, homopolymer poly(9,9-dioctylfluorene) (PFO) (Figure 1a) shows relatively efficient blue electroluminescence [13] and trap-free time-of-flight photocurrent hole transport [14], and was initially of strong interest for display applications. Its high ionization potential, however, limited hole injection from common anode materials [15], spawning a strong interest in alternating fluorene-arylamine copolymers for which ohmic injection could be achieved [16], and leading ultimately to a successfully engineered range of proprietary complex copolymers [17].

Simpler structures that are disclosable can often be used to gain an understanding of the elements of such success, and we focus here on four statistical copolymers with a 9,9-dioctylfluorene (F8) based polymer backbone into which an increasing fraction of butyl-substituted phenylenediamine (BSP) units is incorporated (Figure 1b). For ease, they are hereafter denoted 95F8:5BSP, 90F8:10BSP, 80F8:20BSP, and 50F8:50BSP, corresponding to x % F8:(100 − x) % BSP. Poly(9,9-dioctylfluorene) (i.e., 100F8:0BSP) is a reference point for this study, as also is the alternating copolymer 50F8:50BSP, poly(9,9-dioctylfluorene-alt-bis-N,N′-(4-butylphenyl)-bis-N,N′-phenyl-1,4-phenylenediamine), known in the literature as PFB [18–20].

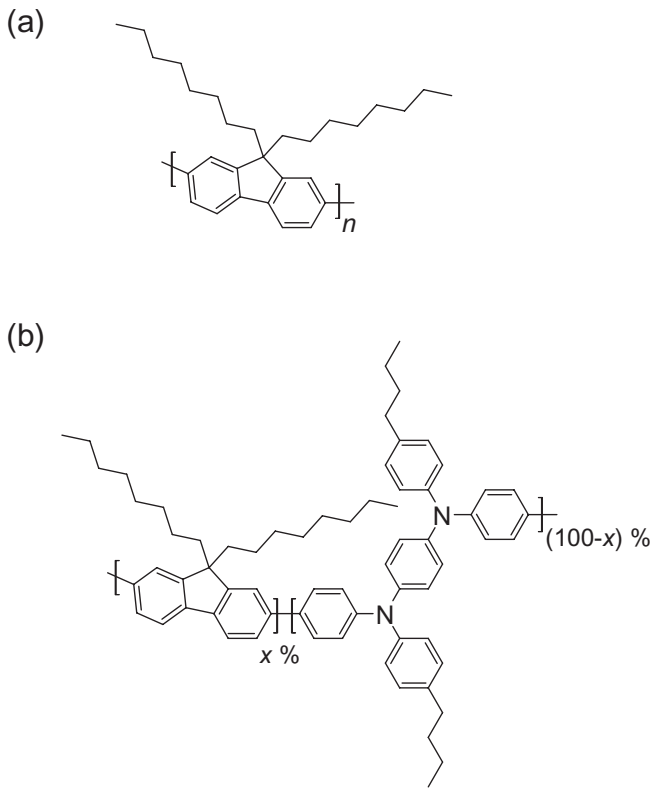

FIGURE 1 | Chemical structures of (a) poly(9,9-dioctylfluorene) and (b) 9,9-dioctylfluorene:butyl-substituted phenylenediamine (F8:BSP) copolymers (x = 95%, 90%, 80%, and 50% for 95F8:5BSP, 90F8:10BSP, 80F8:20BSP, and 50F8:50BSP).

In addition to changes in chemical composition, fluorene-based materials can display a significant variation in physical structure. For PFO, the microstructure can be disordered, liquid crystalline, or (semi-)crystalline, with the added complication of distinct chain segment conformations in the disordered and liquid crystalline phases [13, 21, 22]. These conformations are characterized by different torsion angles between the constituent fluorene units. Glassy-phase PFO is a disordered phase with a large spread of torsion angles (from 120° to 140°). In contrast, the β-phase contains a fraction of highly ordered chain segments with planarized interunit torsion angles of ≈180°. The β-phase can be reliably introduced into an otherwise glassy (disordered or liquid crystalline) PFO film during deposition or via post processing [23]. Spatial patterning is possible in the latter case, allowing the formation of nanostructures [24].

The same process can be utilized to generate β-phase chain segments within fluorene-arylamine copolymers [20], and indeed other fluorene-based copolymers [25, 26] provided there are sufficiently extended sequences of F8 units. β-phase chain segments with their ordered chain-extended geometry result in longer conjugation lengths over which π-electrons can delocalize, leading to lower ionization potential and optical gap. Consequently, both holes and excitons trap on the β-phase chain segments [21]. The presence of β-phase segments is clearly identified through signatures in the UV–Vis absorption and photoluminescence [21, 23]. Additionally, it has been demonstrated that PFO samples containing β-phase segments possess about two orders lower room temperature time-of-flight hole mobility than glassy films [27].

In this study, the dependence of the hole mobility on both copolymer arylamine content and molecular conformation has been investigated using dark injection transient (DIT) measurements. The results are discussed in the context of a transition from trap-limited to trap-to-trap hopping transport. This model is supported by ambient pressure photoemission spectroscopy measurements of the copolymer molecular orbital energies that show different energies for arylamine- and fluorene-based hole sites, for which the relative weight changes with chemical fraction. The observed behavior for the copolymer films studied here is distinct from that for the addition of molecular dopants such as tetraphenyl porphyrin (TPP) to thick PFO films for which the transport becomes highly dispersive [28]. That this is not the case here, even though the ionization potential offset for TPP is significantly smaller than for copolymer BSP moieties, is consistent with thin disordered conjugated copolymers differing in fundamental ways from xerographic blends [18] and polycrystalline materials [19].

2 | Results and Discussion

The primary study of charge carrier transport was performed using the DIT technique, monitoring the current response to a voltage step applied to the injecting contact of diodes comprising indium tin oxide (ITO)/poly(3,4-ethylenedioxythiophene): polystyrene sulphonate (PEDOT:PSS)/F8:BSP copolymer/aluminum (Al). The ITO/PEDOT:PSS anode injects holes, with Al

acting as a blocking contact for electrons. Figure 2a presents typical current transients at a variety of applied voltages for the 50F8:50BSP copolymer, while Figure 2b shows an idealized DIT measurement result. The current response consists of an initial spike at the beginning of the voltage step due to the device capacitance (RC response time, τ). This is followed by the DI transient with a peak at t_{DI}, and at longer times, as the charge distribution tends to dynamic equilibrium, the SCL current (SCLC) density is approached. Care was taken to ensure that the RC time constant is much shorter than t_{DI} so that the transit peak can be clearly resolved. Representative DI hole current transients for both glassy- (Figure S1) and β-phase (Figure S2) samples of 80F8:20BSP, 90F8:10BSP, and 95F8:5BSP are presented in Supporting Information S1: Section A. DI transit times, t_{DI}, are readily identified in all of the transients, confirming that ITO/PEDOT:PSS provides an ohmic injecting contact as expected from the polymer ionization potentials [16].

Figure 3a shows the glassy-phase DIT hole mobilities, extracted from t_{DI} values obtained for the different copolymers, plotted as a function of the square root of the applied electric field. The mobility values deduced for β-phase containing copolymer films are identical, within experimental error, to their glassy counterparts.

It has been shown, using transient microwave conductivity measurements, that the intrachain mobility of individual β-phase PFO polymer chain segments is higher than for the corresponding glassy chain segments [29]. The bulk thin film mobility of β-phase PFO is, nevertheless, lower than for fully glassy films [27]. This seeming anomaly can be explained by recognizing that the extended β-phase chain segments possess less deep-lying highest occupied molecular orbital (HOMO) energies and, thus, when present in moderate numbers, act as "trapping sites" for holes. The hole "trap depth" for β-phase chain segments is ~130 meV [27]. This is significantly less than the corresponding offset for arylamine moieties within xF8:(100 − x)BSP copolymers (*vide infra*) and, as a consequence, the presence or absence of β-phase segments does not significantly affect the arylamine-controlled hole transport in the copolymers.

It does, however, significantly affect the photoluminescence (PL) spectra, as shown for thin film copolymer samples before and after solvent vapor treatment in Figure S3, where the spectrum

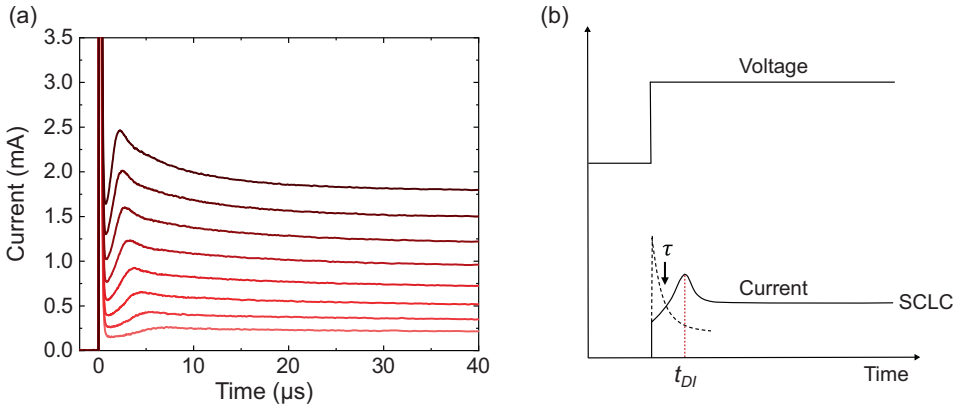

FIGURE 2 | (a) Representative hole injection transients for an 820 nm thick film of 50F8:50BSP under voltage pulses from bottom to top of 5, 6, 7, 8, 9, 10, 11, and 12 V. (b) Idealized representation of the dark injection transient measurement result.

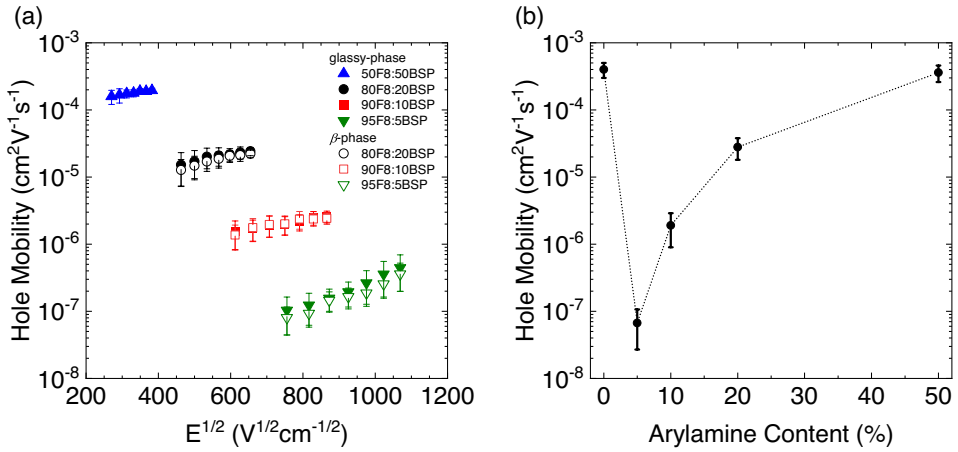

FIGURE 3 | (a) Room temperature, field dependent DIT hole mobility values for films of 50F8:50BSP (blue up-pointing triangles), 80F8:20BSP (black circles), 90F8:10BSP (red squares), and 95F8:5BSP (green down-pointing triangles). The glassy-phase results are represented with filled symbols while the β-phase values are denoted with open symbols. (b) Room temperature hole mobilities for PFO, 95F8:5BSP, 90F8:10BSP, 80F8:20BSP, and 50F8:50BSP at an electric field of 5×10^5 V cm^{-1}. The mobility values for 50F8:50BSP and 80F8:20BSP were extrapolated from the electric field dependence displayed in (a). The dotted lines are a guide to the eye.

for homopolymer PFO is also presented as a reference. These spectra confirm the controlled formation of the β-phase conformation in the copolymers with smaller fractions of BSP, for which there are F8 sequences long enough to support the generation of β-phase chain segments. The characteristic β-phase PL signatures are described in Supporting Information S1: Section B, with deconvolution of the BSP-supported broad charge-transfer (CT) and F8 vibronic-structured neutral exciton contributions for 90F8:10BSP and 95F8:5BSP shown in Figure S4. The alternating copolymer PFB (50F8:50BSP) does not show β-phase features due to the lack of an extended sequence of F8 units [20]. At BSP fractions of 20% or less, however, there are long enough F8 segments present within these statistical copolymers to support β-phase formation, consistent with previous studies that reported the need for a minimum of five F8 repeat units [30]. The transport and emission characteristics are thereby separable, as indeed needed to achieve multifunctional character for state-of-the-art complex copolymers.

Confirmation of the physical nature of this process is provided by the ready removal of the β-phase signatures on heating above the copolymer glass transition temperature. Subsequent solvent vapor treatment restores the β-phase signatures, showing recyclability between β- and glassy-phase. PL spectra recorded for 90F8:10BSP and 95F8:5BSP copolymer films initially in the β-phase, subjected to annealing at increasing temperatures, and then after further solvent vapor treatment are reported in Supporting Information S1: Section C.

In the presence of traps, the DIT peak becomes difficult to resolve when the characteristic trapping time is comparable to the SCL transit time for carriers to cross the sample [31]. The trapping time is a characteristic of the material, while the SCL transit time can be decreased by decreasing the sample thickness and/or increasing the applied field. As the voltage pulses could not be significantly increased in magnitude with our apparatus, the film thicknesses were reduced to ensure that clear DIT traces could be measured in all cases.

The DIT mobility values generally follow Poole–Frenkel behavior [32], with field dependence described by:

$$\mu(E) = \mu_0 \exp\left(\gamma \sqrt{E}\right) \tag{1}$$

where μ_0 is the (extrapolated) zero-field mobility, γ is a parameter that characterizes the strength of the field dependence for a particular material, and E is the applied electric field. Such behavior is common for organic semiconductors as a result of energetic disorder among transport sites [33, 34]. The extracted transport parameters (μ_0 and γ) are summarized in Table 1 together with literature values for PFO.

The copolymer room temperature hole mobility values at an electric field of $5\times10^5\,\mathrm{V\,cm^{-1}}$ (typical for OLED operation) are plotted against arylamine content in Figure 3b. The literature value [14, 27] for the time-of-flight photocurrent mobility of glassy PFO (0% arylamine), namely $4\times10^{-4}\,\mathrm{cm^2\,V^{-1}\,s^{-1}}$, is also presented. Addition of 5% arylamine to form 95F8:5BSP reduces the hole mobility of PFO by some four orders of magnitude to $6.7\times10^{-8}\,\mathrm{cm^2\,V^{-1}\,s^{-1}}$. Then, with increasing arylamine fraction, the mobility increases, reaching $1.9\times10^{-6}\,\mathrm{cm^2\,V^{-1}\,s^{-1}}$ for 90F8:10BSP, $2.8\times10^{-5}\,\mathrm{cm^2\,V^{-1}\,s^{-1}}$ for 80F8:20BSP, and $3.6\times10^{-4}\,\mathrm{cm^2\,V^{-1}\,s^{-1}}$ for 50F8:50BSP. The latter value is in good agreement with previously reported time-of-flight photocurrent values for PFB [18].

The observed mobility changes with arylamine content can be explained in the context of a transition from "trap-and-release" to "arylamine-to-arylamine" hopping controlled SCL transport. Charge transport in disordered organic semiconductors occurs by charge hopping between neighboring transport sites [36, 37]. In a trap-free system, the energetic distribution of hopping sites is governed by the density of states width related to the distribution of molecular conformations and is relatively narrow for fluorene-based polymers, yielding nondispersive time-of-flight photocurrent transients [14]. This pertains also to alternating copolymer fluorene-arylamine systems like PFB [18] and poly(9,9-dioctylfluorene-alt-bis-N,N′-(4-methoxyphenyl)-bis-N,N′-phenyl-1,4-phenylenediamine) (PFMO) [16].

The addition of TPP, with an ionization potential offset of ~0.4 eV, at 5% by weight to thick PFO films leads to trap-limited transport that is highly dispersive [28]. That is not the case here, where the 5% BSP copolymer film still shows a clean DIT trace (Figure S1c) despite there being a significantly larger expected offset of ~0.7 eV for BSP relative to F8 units. This is consistent with disordered conjugated copolymers differing in fundamental ways from both traditional xerographic blends [18] and polycrystalline materials [19].

For 95F8:5BSP the sparse BSP units do control hole transport, severely limiting mobility, but samples can still be prepared that display SCL behavior. As the fraction of BSP units increases, the mobility increases due to BSP-to-BSP hopping [38, 39]. The charge carriers can then increasingly percolate among BSP sites rather than have to make energy-consuming jumps to transport among the F8 sites.

TABLE 1 | Transport parameters deduced for fluorene-arylamine copolymers and PFO.

Material	μ_0 ($\mathrm{cm^2\,V^{-1}\,s^{-1}}$)	γ ($\mathrm{cm^{1/2}\,V^{-1/2}}$)	References
PFO	3×10^{-4}	0.2×10^{-3}	[35]
50F8:50BSP	$(1.0\pm0.1)\times10^{-4}$	$(1.7\pm0.2)\times10^{-3}$	This work
80F8:20BSP	$(6.3\pm0.8)\times10^{-6}$	$(2.1\pm0.2)\times10^{-3}$	This work
90F8:10BSP	$(4.2\pm0.5)\times10^{-7}$	$(2.1\pm0.2)\times10^{-3}$	This work
95F8:5BSP	$(2.3\pm0.6)\times10^{-9}$	$(4.9\pm0.3)\times10^{-3}$	This work

Air photoemission spectroscopy (APS) experiments allow direct measurement of the ionization onsets of molecular sites present within the copolymer films. As already noted, from cyclic voltammetry (CV) measurements, PFB [18] has a significantly lower electrochemical ionization potential (~5.1 eV) than that found for PFO (~5.8 eV) [15] and as a consequence, one might expect to see significant changes in the APS data through the introduction of BSP units into the F8:BSP copolymer structures.

The APS ionization onset values are obtained—using the expected current variation—from plots of the cube root of the photoemission current against photon energy [40–42]. The linear portion of the increasing current curve allows determination of the onset by extrapolation to the baseline signal. The APS data for glassy films of F8:BSP copolymers and PFO are presented in Figure 4a and Figure S9a and the obtained ionization onsets for PFO and PFB are in broad agreement with literature values [15, 18, 20].

For the lower mobility copolymers, i.e., 95F8:5BSP, 90F8:10BSP, and 80F8:20BSP, the photoemission onset is significantly below a straight line extrapolation between the PFO and PFB onsets. This is consistent with the presence of electronic states within the gap for these materials. Two different species then contribute to the measured photoemission signal; the lower energy onset is assigned to trap states associated with BSP units within an otherwise F8 chain segment, while the higher energy component is dominated by the ionization of F8 segments themselves.

Similar behavior has been reported previously in APS measurements of individual polymers and polymer blend films [43] as well as small-molecule donor/acceptor blends [44], with the signal below the expected HOMO level associated with sub-gap states. Copolymer samples containing β-phase F8 segments also showed similar behavior, with two photoemission contributions (Figure 4b and Figure S9b).

CV measurements of the 95F8:5BSP copolymer show two oxidation peaks as well, analogous to the two APS contributions [20]. The higher energy CV peak was also previously assigned to F8 oxidation, while the second peak situated ~0.3 eV lower in energy—similar to the photoemission threshold offset seen here—was attributed to the preferential oxidation of BSP units. Miteva et al. [45] likewise reported two CV peaks for triarylamine end-capped polyfluorenes, at 5.48 and 5.88 eV for the triarylamine and fluorene moieties, respectively. These end groups are considered to act as independent electroactive units and to constitute hole traps within the majority fluorene-composed films.

The measured APS intensity reflects a gradual increase in the population of lower energy states with increasing BSP concentration until they form a well-defined lower energy transport level at 5.15 eV for 50F:50BSP. The photoemission thresholds shift to lower energies with increasing arylamine content as expected when hybridization occurs between the F8 and arylamine moieties (Figure S10). At 50% BSP, a single energy level is formed via which charge carrier transport takes place.

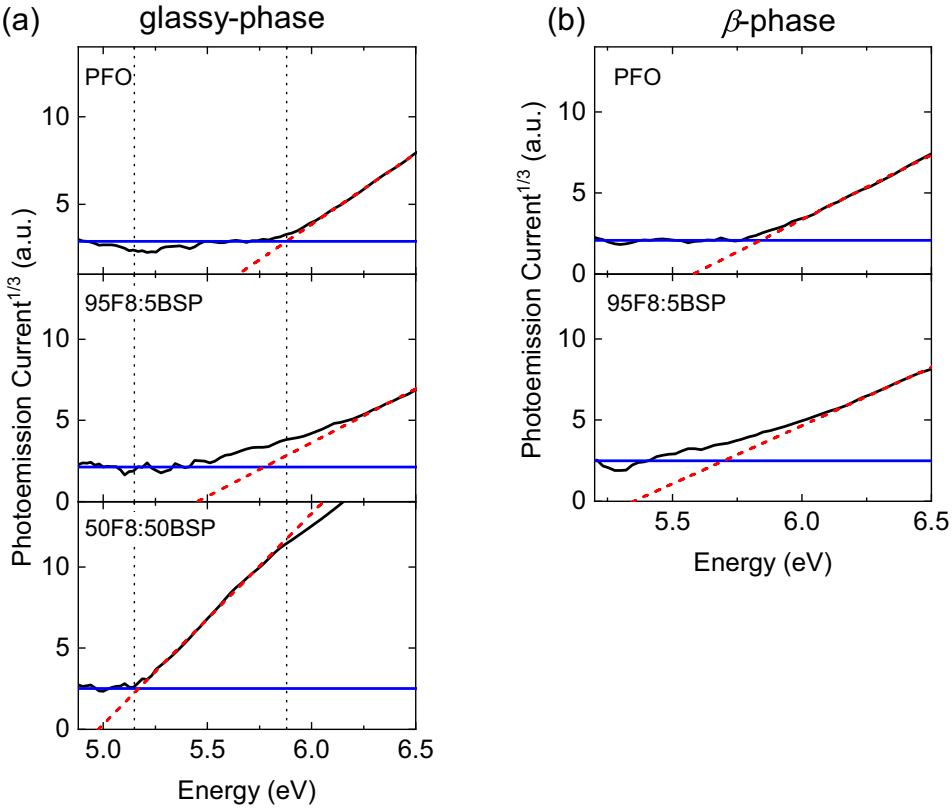

FIGURE 4 | Air photoemission spectroscopy data (black line) for (a) glassy-phase PFO, 95F8:5BSP, and 50F8:50BSP and (b) β-phase PFO, 95F8:5BSP. The ionization onsets are determined by extrapolating the linear parts of each curve (see representative red dashed lines) to their respective baseline signal levels (blue horizontal lines). The vertical dashed lines at 5.15 and 5.88 eV provide visual guides to the onsets for glassy-phase PFB and PFO, respectively. The 95F8:5BSP signals for both glassy- and β-phase samples show onsets significantly below the respective PFO energies and two slopes indicative of two ionisable species.

How the photoemission onset extracted from APS is related to the true trap depth and the disorder parameter value in a material is an interesting direction for future investigation. Exploring the potential of the APS technique for studying charge trapping deserves further attention. This measurement method does not require vacuum conditions or low temperatures, significantly reducing experimental efforts compared to more commonly used charge trapping experiments, but its interpretation for molecular materials needs further study.

Due to trapping at arylamine sites, the hole charge carrier mobility for low BSP concentration copolymers is markedly lower than the 100% F8 polymer (PFO). The mobility then increases as the BSP concentration increases due to direct arylamine–arylamine hopping. The hopping rate between two sites depends on the electronic coupling between the sites due to wavefunction overlap and, thus, on the inter-site distance and relative orientation of molecular orbitals (Miller and Abrahams model) [46]. As the concentration of BSP increases, the BSP–BSP inter-site distance reduces and eventually, when large arylamine concentrations are present, the transport proceeds mainly via the BSP-localized states. The field dependence of the mobility correspondingly decreases with increasing BSP fraction (c.f. γ-values in Table 1), in accordance with the correlated disorder model [19, 33, 34, 47]. Similar observations have been made for organic semiconductor films deliberately doped with molecular trapping units [28, 38, 48–50].

3 | Conclusions

The hole transport properties of four fluorene-arylamine copolymers comprising different ratios of 9,9-dioctylfluorene (F8) and butyl-substituted phenylenediamine (BSP) have been investigated as model systems for the design of complex copolymers. Samples with BSP fractions of 50%, 20%, 10%, and 5% were studied. The hole mobility of PFO ($4\times10^{-4}\,cm^2V^{-1}s^{-1}$) [14, 27] is drastically reduced by the copolymerization of only 5% BSP, and the resulting 95F8:5BSP copolymer has a mobility ($6.7\times10^{-8}\,cm^2V^{-1}s^{-1}$) some four orders of magnitude lower than PFO. With an increasing percentage of arylamine moieties, the charge transport then improves, and the alternating copolymer 50F8:50BSP has a mobility ($3.6\times10^{-4}\,cm^2V^{-1}s^{-1}$) similar to that of the homopolymer.

This behavior is interpreted as arising from a transition from transport via the F8 units accompanied by trapping at the BSP sites to transport among the BSP moieties. The BSP-to-BSP transport sets in with increasing arylamine concentration as the BSP–BSP inter-site distance becomes sufficiently small for easy hopping to occur. Thus, at high "trap" concentrations transport through the "trap" state manifold becomes possible.

Additionally, the influence of chain conformation on the measured hole mobility is explored, and it is shown that while β-phase formation strongly affects the emission properties, the copolymer films have very similar hole mobilities for both glassy- and β-phase samples. The copolymer room temperature hole transport properties are predominantly determined by arylamine content, but the light emission properties can be independently tuned. In the context of organic light-emitting diodes, this allows optimization of color gamut, efficiency, and lifetime [13, 20]. Our results help, thereby, to elucidate how the complex copolymer approach has proven so beneficial, with separable tuning of different device-relevant physical characteristics [17].

Air photoemission spectroscopy measurements confirmed the presence of BSP-moiety associated sub-gap trap states for the 95F8:5BSP, 90F8:10BSP, and 80F8:20BSP copolymers. APS measurements are performed at room temperature without requiring vacuum conditions. This significantly reduces experimental efforts compared to more commonly used charge trapping experiments and highlights its potential for studying trap and transport states in organic semiconductors. Future work should explore further the APS technique's promise for mapping the transport and trap state landscape of a material, increased energy resolution, and/or quantifying the relative proportions of the states that it detects.

4 | Experimental Section

4.1 | Materials

The PFO homopolymer was purchased from 1-Material Inc. (weight-average molecular weight (M_w) = $55\times10^3\,g\,mol^{-1}$ and polydispersity index (PDI) = 2.5) and used as received. The copolymers were provided by the Sumitomo Chemical Company Tsukuba Research Laboratory and used as supplied. Their M_w values were $260\times10^3\,g\,mol^{-1}$ for 95F8:5BSP, $330\times10^3\,g\,mol^{-1}$ for 90F8:10BSP, $110\times10^3\,g\,mol^{-1}$ for 80F8:20BSP, and $300\times10^3\,g\,mol^{-1}$ for 50F8:50BSP.

4.2 | Photoluminescence Spectroscopy

Thin films were spin coated at 2000 rpm from $10\,mg\,mL^{-1}$ toluene solutions onto quartz (Spectrosil B) substrates. A Dektak Systems surface profilometer was used to measure the resulting film thickness, typically ~70 nm. For the preparation of glassy-phase films, both solution vials and substrates were placed on a hot plate at 100°C for 5 min immediately prior to spin coating. For β-phase samples, solvent vapor annealing of glassy films was employed. This was done via exposure to toluene vapor at room temperature for 12 h, with film swelling generating the mechanical stress that drives planarization of a fraction of the polymer chains [51]. We follow the convention in the literature that samples containing such a fraction of β-phase chains in an otherwise glassy film are called β-phase samples, irrespective of the specific fraction. The same procedures were used for the fabrication of all glassy-phase and β-phase films used in this study. PL spectra were recorded in reflection geometry using a Jobin Yvon Horiba Fluoromax-3 spectrofluorometer (370 nm excitation) in ambient air.

4.3 | Dark Injection Transient Measurement

DIT experiments were carried out using a Fluxim PAIOS measurement platform. Diodes with the structure ITO/PEDOT:PSS/Copolymer/Al were fabricated for the measurements of hole charge carrier mobility. Commercial (Luminescence Technology

Corporation) ITO-coated glass substrates with a typical resistance of 20 $\Omega\square^{-1}$ were employed. A 40 nm thick film of PEDOT:PSS (Clevios P VP AI 4083) was deposited as an ohmic hole-injecting layer by spin coating at 3000 rpm and annealing in air for 20 min at 150°C. The copolymers were spin coated on top of the PEDOT:PSS layer at 2000 rpm from toluene solutions (10–60 mg mL^{-1}). The preparation of glassy-phase and β-phase films was carried out following the same procedure used for the photoluminescence spectroscopy samples. Finally, aluminum electrodes of 70 nm thickness were deposited onto the copolymer films, yielding sandwich structures with an active area, defined by the electrode overlap, of 25 mm^2. The copolymer film thickness values were 105 nm for 95F8:5BSP, 160 nm for 90F8:10BSP, 280 nm for 80F8:20BSP, and 820 nm for 50F8:50BSP, adjusted to ensure a suitable time window for the transient peak as the mobility increased with increasing arylamine content.

4.4 | Air Photoemission Spectroscopy

Air photoemission spectroscopy (APS) is a technique used to determine the molecular orbital energies of organic semiconductors. Its mode of operation is based on the photoelectric effect, measuring the number of photoelectrons emitted from a sample when illuminated by a tuneable monochromatic UV light source. Photoemission occurs when the photon energy exceeds the material's ionization potential, allowing the ionization potential to be determined by scanning the excitation photon energy while measuring the resulting photoemission current.

Most photoemission spectroscopy techniques require measurements under vacuum, as the electron mean free path at ambient pressure (1–3 μm) is too short for electrons to reach the detector [40]. In APS, however, photoelectrons emitted under ambient conditions are quickly stopped near the sample surface, forming a localized charge cloud. This leads to the generation of atmospheric ions. While the kinetic energy information of the electrons is lost, their electronic charge is conserved. These ions, having significantly longer mean free paths than electrons, can migrate toward a detector tip when a potential is applied, generating a measurable current. This enables an indirect measurement of the photoemission current and hence the ionization potential of energy levels within the organic semiconductor film. The technique is widely used as an alternative to cyclic voltammetry electrochemical measurements. The latter are performed with the film immersed in an electrolyte, subject to counter ion interactions, and requiring an empirical correction factor to determine the ionization potential [15].

Samples were prepared as 100 nm thickness films spin-coated from toluene solution (15 mg mL^{-1}) on precleaned ITO-coated glass substrates. Glassy-phase and β-phase films were prepared using the same process as for the photoluminescence spectroscopy samples. Ionization potential determinations were performed using air photoemission spectroscopy with a KP Technology APS-04 system. The tip was held at an average height of 1 mm above the sample surface and at a potential difference of +10 V relative to the underlying ITO electrode. The sample was simultaneously illuminated with a 4–5 mm diameter light spot, provided by the monochromated output from a broadband (4–7 eV) deuterium lamp source. Increasing the incident photon energy leads to the onset of photocurrent when charges are excited from the sample. Straight line fits to the increasing photocurrent slope were used to identify onset energies from which ionization potential values were deduced.

Acknowledgments

Nikol T. Lambeva and Donal D.C. Bradley acknowledge studentship funding from the UK Engineering and Physical Sciences Research Council [grant number 1734270] together with equipment funding from Oxford University. The authors would like to thank Dr. Toshihiro Ohnishi and Mr. Takeshi Yamada of the Sumitomo Chemical Company Tsukuba Research Laboratory for supplying the dioctylfluorene-arylamine copolymers.

References

1. J. H. Burroughes, D. D. C. Bradley, A. R. Brown, et al., "Light-Emitting Diodes Based on Conjugated Polymers," *Nature* 347 (1990): 539–541.

2. G. Yu, J. Gao, J. C. Hummelen, F. Wudl, and A. J. Heeger, "Polymer Photovoltaic Cells: Enhanced Efficiencies via a Network of Internal Donor–Acceptor Heterojunctions," *Science* 270 (1995): 1789–1791.

3. J. Song, H. Liu, Z. Zhao, P. Lin, and F. Yan, "Flexible Organic Transistors for Biosensing: Devices and Applications," *Advanced Materials* 36 (2023): 2300034.

4. F. Le Roux, A. Mischok, D. D. C. Bradley, and M. C. Gather, "Efficient Anisotropic Polariton Lasing Using Molecular Conformation and Orientation in Organic Microcavities," *Advanced Functional Materials* 32 (2022): 220941.

5. P. O. Morin, T. Bura, and M. Leclerc, "Realizing the Full Potential of Conjugated Polymers: Innovation in Polymer Synthesis," *Materials Horizons* 3 (2016): 11–20.

6. B. M. T. Bernius, M. Inbasekaran, J. O. Brien, and W. Wu, "Progress With Light-Emitting Polymers," *Advanced Materials* 12 (2000): 1737–1750.

7. F. R. Mayo and C. Walling, "Copolymerization," *Chemical Reviews* 46 (1950): 191–287.

8. J. S. Kim, P. K. H. Ho, C. E. Murphy, and R. H. Friend, "Phase Separation in Polyfluorene-Based Conjugated Polymer Blends: Lateral and Vertical Analysis of Blend Spin-Cast Thin Films," *Macromolecules* 37 (2004): 2861–2871.

9. B. K. Yap, R. Xia, M. Campoy-Quiles, P. N. Stavrinou, and D. D. C. Bradley, "Simultaneous Optimization of Charge-Carrier Mobility and Optical Gain in Semiconducting Polymer Films," *Nature Materials* 7 (2008): 376–380.

10. H. Bässler and A. Köhler, "Charge Transport in Organic Semiconductors," *Topics in Current Chemistry* 312 (2012): 1–65.

11. S. Fratini, M. Nikolka, A. Salleo, G. Schweicher, and H. Sirringhaus, "Charge Transport in High-Mobility Conjugated Polymers and Molecular Semiconductors," *Nature Materials* 19 (2020): 491–502.

12. Y. Olivier, D. Niedzialek, V. Lemaur, et al., "25th Anniversary Article: High-Mobility Hole and Electron Transport Conjugated Polymers: How Structure Defines Function," *Advanced Materials* 26 (2014): 2119–2136.

13. A. W. Grice, D. D. C. Bradley, M. T. Bernius, M. Inbasekaran, and E. P. Woo, "High Brightness and Efficiency Blue Light-Emitting Polymer Diodes," *Applied Physics Letters* 73, no. 5 (1998): 629–631.

14. M. Redecker, D. D. C. Bradley, M. Inbasekaran, and E. P. Woo, "Non-dispersive Hole Transport in an Electroluminescent Polyfluorene," *Applied Physics Letters* 73 (1998): 1565–1567.

15. S. Janietz, D. D. C. Bradley, M. Grell, C. Giebeler, M. Inbasekaran, and E. P. Woo, "Electrochemical Determination of the Ionization Potential and Electron Affinity of Poly(9,9-Dioctylfluorene)," *Applied Physics Letters* 73 (1998): 2453–2455.

16. A. J. Campbell, D. D. C. Bradley, H. Antoniadis, M. Inbasekaran, W. W. Wu, and E. P. Woo, "Transient and Steady-State Space-Charge-Limited Currents in Polyfluorene Copolymer Diode Structures With Ohmic Hole Injecting Contacts," *Applied Physics Letters* 76 (2000): 1734–1736.

17. C. Sekine, Y. Tsubata, T. Yamada, M. Kitano, and S. Doi, "Recent Progress of High Performance Polymer OLED and OPV Materials for Organic Printed Electronics," *Science and Technology of Advanced Materials* 15 (2014): 034203.

18. M. Redecker, D. D. C. Bradley, M. Inbasekaran, W. W. Wu, and E. P. Woo, "High Mobility Hole Transport Fluorene-Triarylamine Copolymers," *Advanced Materials* 11 (1999): 241–246.

19. A. J. Campbell, R. Rawcliffe, A. Guite, et al., "Charge-Carrier Density Independent Mobility in Amorphous Fluorene-Triarylamine Copolymers," *Advanced Functional Materials* 26 (2016): 3720–3729.

20. I. Hamilton, N. Chander, N. J. Cheetham, et al., "Controlling Molecular Conformation for Highly Efficient and Stable Deep-Blue Copolymer Light-Emitting Diodes," *ACS Applied Materials & Interfaces* 10, no. 13 (2018): 11070–11082.

21. M. Ariu, M. Sims, M. D. Rahn, et al., "Exciton Migration in β-Phase Poly(9,9-Dioctylfluorene)," *Physical Review B: Condensed Matter and Materials Physics* 67 (2003): 1.

22. M. Grell, D. D. C. Bradley, G. Ungar, J. Hill, and K. S. Whitehead, "Interplay of Physical Structure and Photophysics for a Liquid Crystalline Polyfluorene," *Macromolecules* 32 (1999): 5810–5817.

23. A. Perevedentsev, N. Chander, J. S. Kim, and D. D. C. Bradley, "Spectroscopic Properties of Poly(9,9-Dioctylfluorene) Thin Films Possessing Varied Fractions of β-Phase Chain Segments: Enhanced Photoluminescence Efficiency Via Conformation Structuring," *Journal of Polymer Science Part B: Polymer Physics* 54 (2016): 1995.

24. A. Perevedentsev, Y. Sonnefraud, C. R. Belton, et al., "Dip-Pen Patterning of Poly(9,9-Dioctylfluorene) Chain-Conformation-Based Nano-Photonic Elements," *Nature Communications* 6, no. 1 (2015): 1, 5977.

25. B. Wang, H. Ye, M. Riede, and D. D. C. Bradley, "Chain Conformation Control of Fluorene-Benzothiadiazole Copolymer Light-Emitting Diode Efficiency and Lifetime," *ACS Applied Materials & Interfaces* 13 (2021): 2919.

26. N. T. Lambeva, C. C. Mullen, X. Gao, et al., "Conformation Control of Triplet State Diffusion in Platinum Containing Polyfluorene Copolymers," *Journal of Polymer Science* 61 (2023): 83–93.

27. S. Foster, *On the Influence of Physical and Chemical Structure on Charge Transport in Disordered Semiconducting Materials and Devices* (Imperial College of Science, Technology and Medicine, 2013).

28. A. J. Campbell, D. D. C. Bradley, T. Virgili, D. G. Lidzey, and H. Antoniadis, "Improving Efficiency by Balancing Carrier Transport in Poly(9,9-Dioctylfluorene) Light-Emitting Diodes Using Tetraphenylporphyrin as a Hole-Trapping, Emissive Dopant," *Applied Physics Letters* 79 (2001): 3872–3874.

29. P. Prins, F. C. Grozema, B. S. Nehls, T. Farrell, U. Scherf, and L. D. A. Siebbeles, "Enhanced charge-carrier mobility in β -phase polyfluorene," *Physical Review B: Condensed Matter and Materials Physics* 74 (2006): 10.

30. W. C. Tsoi, A. Charas, A. J. Cadby, et al., "Observation of the β-Phase in Two Short-Chain Oligofluorenes," *Advanced Functional Materials* 18 (2008): 600–606.

31. A. Many and G. Rakavy, "Theory of Transient Space-Charge-Limited Currents in Solids in the Presence of Trapping," *Physics Review* 1962 (1980): 126–1988.

32. W. D. Gill, "Drift Mobilities in Amorphous Charge-Transfer Complexes of Trinitrofluorenone and Poly-n-Vinylcarbazole," *Journal of Applied Physics* 43 (1972): 5033–5040.

33. S. V. Novikov, D. H. Dunlap, V. M. Kenkre, P. E. Parris, and A. V. Vannikov, "Essential Role of Correlations in Governing Charge Transport in Disordered Organic Materials," *Physical Review Letters* 81 (1998): 4472–4475.

34. Y. N. Gartstein and E. M. Conwell, "High-Field Hopping Mobility in Molecular Systems With Spatially Correlated Energetic Disorder," *Chemical Physics Letters* 245 (1995): 351–358.

35. H. H. Fong, A. Papadimitratos, and G. G. Malliaras, "Nondispersive Hole Transport in a Polyfluorene Copolymer With a Mobility of $0.01\,cm^2V^{-1}s^{-1}$," *Applied Physics Letters* 89 (2006): 87.

36. H. Bässler, "Charge Transport in Disordered Organic Photoconductors a Monte Carlo Simulation Study," *Physica Status Solidi* 175 (1993): 15–56.

37. V. I. Arkhipov, I. I. Fishchuk, A. Kadashchuk, and H. Bässler, *Semiconducting Polymers: Chemistry, Physics and Engineering* (Wiley-VCH Verlag GmbH, 2007).

38. I. I. Fishchuk, A. K. Kadashchuk, A. Vakhnin, et al., "Transition From Trap-Controlled to Trap-to-Trap Hopping Transport in Disordered Organic Semiconductors," *Physical Review B: Condensed Matter and Materials Physics* 73 (2006): 1.

39. I. I. Fishchuk, A. K. Kadashchuk, H. Bässler, and D. S. Weiss, "Non-dispersive charge-carrier transport in disordered organic materials containing traps," *Physical Review B: Condensed Matter and Materials Physics* 66 (2002): 1.

40. I. D. Baikie, A. C. Grain, J. Sutherland, and J. Law, "Dual Mode Kelvin Probe: Featuring Ambient Pressure Photoemission Spectroscopy and Contact Potential Difference," *Energy Procedia* 60 (2014): 48–56.

41. I. D. Baikie, A. Grain, J. Sutherland, and J. Law, "Near Ambient Pressure Photoemission Spectroscopy of Metal and Semiconductor Surfaces," *Physica Status Solidi C: Current Topics in Solid State Physics* 12 (2015): 259.

42. J. R. Harwell, T. K. Baikie, I. D. Baikie, et al., "Probing the Energy Levels of Perovskite Solar Cells via Kelvin Probe and UV Ambient Pressure Photoemission Spectroscopy," *Physical Chemistry Chemical Physics* 18 (2016): 19738–19745.

43. C. Labanti, J. Wu, J. Shin, et al., "Light-Intensity-Dependent Photoresponse Time of Organic Photodetectors and its Molecular Origin," *Nature Communications* 13, no. 1 (2022): 3745,.

44. J. Wu, J. Lee, Y. C. Chin, et al., "Exceptionally Low Charge Trapping Enables Highly Efficient Organic Bulk Heterojunction Solar Cells," *Energy & Environmental Science* 13 (2020): 2422–2430.

45. T. Miteva, A. Meisel, W. Knoll, et al., "Improving the Performance of Polyfluorene-Based Organic Light-Emitting Diodes via End-Capping," *Advanced Materials* 13 (2001): 565–570.

46. A. Miller and E. Abrahams, "Impurity Conduction at Low Concentrations," *Physics Review* 120 (1960): 745–755.

47. D. H. Dunlap, P. E. Parris, and V. M. Kenkre, "Charge-Dipole Model for the Universal Field Dependence of Mobilities in Molecularly Doped Polymers," *Physical Review Letters* 77 (1996): 542–545.

48. D. M. Pai, J. F. Yanus, and M. Stolka, "Trap-Controlled Hopping Transport," *Journal of Physical Chemistry* 88 (1984): 4714–4717.

49. P. M. Borsenberger, E. H. Magin, and S. A. Visser, "Charge Trapping in Molecularly Doped Polymers," *Japanese Journal of Applied Physics, Part 1: Regular Papers & Short Notes* 37 (1998): 1945.

50. P. M. Borsenberger, W. T. Gruenbaum, E. H. Magin, D. E. Schildkraut, and S. A. Visser, "Hole Trapping in Molecularly Doped Polymers: The Hoesterey-Letson Formalism," *Japanese Journal of Applied Physics, Part 1: Regular Papers & Short Notes* 38 (1999): 117.

51. M. Ariu, D. G. Lidzey, M. Sims, A. J. Cadby, P. A. Lane, and D. D. C. Bradley, "The Effect of Morphology on the Temperature-Dependent Photoluminescence Quantum Efficiency of the Conjugated Polymer Poly(9, 9-Dioctylfluorene)," *Journal of Physics. Condensed Matter* 14 (2002): 9975–9986.

Supporting Information

Additional supporting information can be found online in the Supporting Information section.